CHARACTERIZATION OF BI-DIRECTIONALLY OSCILLATING DYNAMIC FLOW AND FREQUENCY-DEPENDENT RECTIFICATION PERFORMANCE OF MICRODIFFUSERS

Young-Ho Lee, Tae Goo Kang and Young-Ho Cho

Micromachines and Microsystems Laboratory
Department of Mechanical Engineering
Korea Advanced Institute of Science and Technology
373-1 Kusong-dong, Yusong-ku, Taejon 305-701, Republic of Korea
Phn: +82-42-869-3038 / Fax: +82-42-869-3050 / E-mail: mems@kaist.ac.kr

ABSTRACT

This paper characterizes a bi-directionally oscillating dynamic flow in a planar microdiffuser in order to evaluate the flow rectification performance of the microdiffuser. In the theoretical study, we present a bi-directionally oscillating flow model, where the boundary layer thickness governs the flow rectification performance of the microdiffuser. In the experimental study, we fabricate two different microdiffuser prototypes, having the neck widths of 100μm (D100) and 300μm (D300), respectively. The prototypes, D100 and D300, show the maximum net flow rates of 116.6μl/min and 344.4μl/min, respectively, for an identical piezoelectric flow actuation using the sinusoidal drive voltage of 100Vp-p at 50Hz. The flow rates measured from D100 and D300 are approximately 47% of the theoretical values estimated from the conventional uni-directional flow model for the net boundary layer thicker than the neck width. The experimental flow rate of D300, however, decreases from 47% of the theoretical values at the flow frequencies higher than 90Hz, at which the net boundary layer thickness is reduced to the microdiffuser neck width. It is experimentally verified that the flow rectification performance and the net flow rate of the microdiffuser tend to decrease when the boundary layer thickness is smaller than the diffuser neck width.

INTRODUCTION

Recently, flow-rectifying microdevices [1-9] have received a growing interest for applications to chemical and biomedical analysis systems [10, 11], and have included microcheck valves [1-5] and valveless microdiffusers [6-9]. Among them, the microdiffusers [6-9] have received more attention than the microcheck valves [1-5] due to the advantages of simple structure, high reliability, long lifetime and low cost.

The previous microdiffuser research [1-5] was conducted based on the unidirectional flow model, where the flow passing through the microdiffuser. In this paper, however, we consider a bi-directionally oscillating dynamic flow in the microdiffuser, thereby evaluating the net flow rate and the frequency-dependent rectification performance of the microdiffusers.

THEORETICAL ANALYSIS

Uni-directional Steady Flow

Figure 2 shows the top views of a planar microdiffuser. In the previous study [1-5], the microdiffusers are analyzed by an uni-directional flow model. The pressure loss coefficient, ξ, for the diffuser element is defined [7] as

$$\xi = 2\frac{\Delta P}{\rho \bar{u}^2} \tag{1}$$

where $\bar{u}$ is the mean velocity in the diffuser neck, ρ is the fluid density and ΔP is the pressure drop across the diffuser.

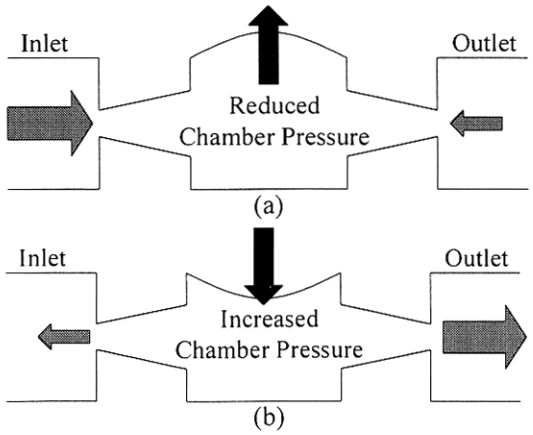

Figure 1. Flow rectifying microdiffusers: (a) In-take cycle reduces chamber pressure by increasing the chamber volume; (b) Out-take cycle increases chamber pressure by decreasing the chamber volume.

For a flow rectification, the pressure loss coefficient in the diffuser flow direction has to be lower than in the nozzle flow direction. This condition can be expressed [8] by the diffuser efficiency ratio, η, greater than 1.

$$\eta = \frac{\xi_{nozzle}}{\xi_{diff}} > 1 \tag{2}$$

where ξ_{nozzle} and ξ_{diff} are the pressure loss coefficient in the diffuser flow direction and in the nozzle flow direction.

From Eq.1 and the microdiffuser inlet area, A_1, we find that

$$\Delta P = \frac{\rho \xi}{2} u_1^2 = \frac{\rho \xi}{2A_1^2} Q_1^2 \tag{3}$$

Thus the flow rate, Q, is obtained as

$$Q = \beta \sqrt{\Delta P} \tag{4}$$

where

$$\beta = A_1 \sqrt{\frac{2}{\rho \xi}} \tag{5}$$

The net flow per unit cycle is expressed as

$$Q_{estimated} = (\beta_1 - \beta_2) \sqrt{\Delta P} \tag{6}$$

where β_1 is diffuser flow direction coefficient and β_2 is nozzle flow direction coefficient, expressed by

$$\beta_1 = A_1 \sqrt{\frac{2}{\rho \xi_{diff}}} \tag{7}$$

$$\beta_2 = A_1 \sqrt{\frac{2}{\rho \xi_{nozzle}}} \tag{8}$$

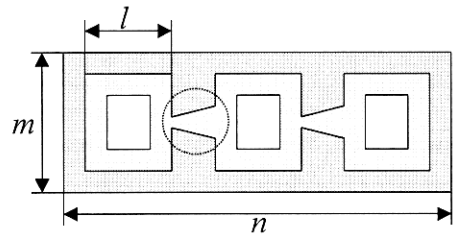

(a)

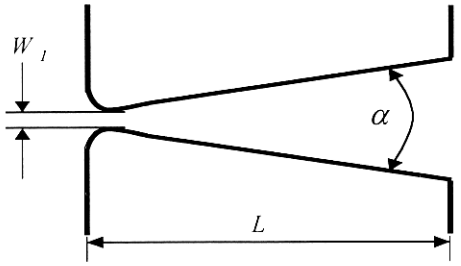

diffuser flow ⇒
nozzle flow ⇐

(b)

Figure 2. Three chambers connected by microdiffusers: (a) Top view; (b) Enlarged view of a microdiffuser, whose dimensions are listed in Table 1.

Bi-directional Oscillating Flow

The previous diffuser flow analysis has been based on stationary flow condition. For the oscillatory pumping of the fluid through the microdiffuser, however, the pressure and flow direction can be rapidly changing. In this case, we have made a hypothesis that the key parameter, affecting the flow rectification performance of the microdiffuser, is the thickness of the boundary layers developed by the bi-directionally oscillating flow in the microdiffuser. Thus, the flow rectification efficiency, estimated from the conventional static flow model, would be valid only for the total boundary layer thickness larger than the neck width of the microdiffuser. For the total boundary layer thickness smaller than the diffuser neck width, however, the flow rectification efficiency would be decreased than the value expected in the static flow model.

The boundary layer thickness at the microdiffuser wall can be estimated by the Stokes' second problem [13]:

$$\frac{\partial u}{\partial t} = \nu \frac{\partial^2 u}{\partial y^2} \tag{9}$$

where ν is kinematic viscosity and y is normal distance from the microdiffuser wall. For the oscillating frequency, ω, the velocity profile along the diffuser wall is given [13] by

$$\frac{u(y,t)}{U} = \exp(-\sqrt{\frac{\omega}{2\nu}} y) \cos(\omega t - \sqrt{\frac{\omega}{2\nu}} y) \tag{10}$$

The penetration depth, δ, where the amplitude of motion, u, is $1/e^2$ of its maximum value, U, is obtained from Eq.10 as follows.

$$\delta = 2\sqrt{\frac{2\nu}{\varpi}} \tag{11}$$

The penetration depth, δ, for water (ν=10^{-6} m/sec^2) is estimated in Fig.3 for varying flow frequency. We consider that the fluid at $y>\delta$ is essentially unaffected by the fluid viscosity.

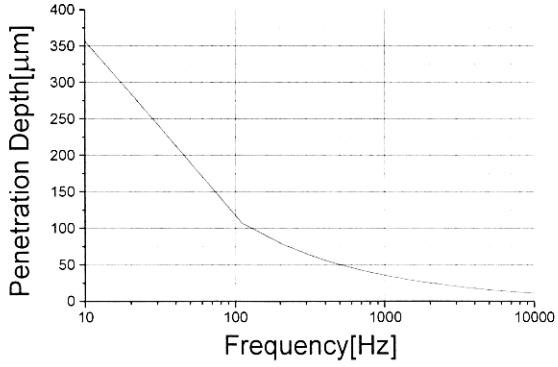

Figure 3. Boundary layer thickness estimated by Stokes' second problem for varying oscillating flow frequency.

Table 1. Dimensions of the microdiffuser prototypes of Fig. 2(b).

Diffuser Prototype	Neck width (W_1) [μm]	Length (L) [μm]	Depth (b) [μm]	Divergence angle (α) [°]
D100	100	1370	40	7
D300	300	4110	40	7

MICRODIFFUSER PROTOTYPES

The diffuser neck width, W_1, is the most important parameter of the microdiffuser. Based on the Stokes' second problem solution, we decided the neck width as 100μm(D100) and 300μm(D300) so that the boundary layer thickness, δ, are 50μm and 150μm at 500Hz and 75Hz respectively. In other words, we decided the neck width as twice times larger than the boundary layer thickness. The divergence angle and the dimensionless length, L/W_1, are selected [9] as 7° and 13.7, respectively. Thus, the diffuser length, L, is decided as 1370μm and 4110μm for the D100 and D300, respectively. The depth, b, is decided as 40μm, and the flow in the vertical direction is considered to be fully developed upto 500Hz. Table 2 shows the summarized dimensions of the designed microdiffusers, where l=8mm, m=16mm and n=40mm.

The microfabrication process is shown in Fig. 4. The microdiffuser fabrication starts with 4″ (100) 520μm-thick silicon wafer. In Fig. 4(a), the silicon wafer is cleaned and thermally oxidized to form a 1.5μm-thick wet silicon dioxide layer as the mask layer for silicon RIE process. In Fig. 4(b), the silicon dioxide layer is patterned by RIE process. After PR strip, microdiffusers and chambers are defined by the silicon deep-RIE process. In Fig. 4(c), the removal of thermal silicon dioxide in BOE is followed by growth of the 2000Å-thick silicon nitride layer by LPCVD. After the silicon nitride layer is patterned by RIE process(Fig. 4(d)), the silicon wafer is etched in KOH solution(Fig. 4(e)). Finally, silicon nitride layer is removed by boiling in H_3PO_4(Fig. 4(f)). Figure 5 shows the SEM photograph of the fabricated microdiffuser.

EXPERIMENTAL SETUP

Figure 6 shows the experimental setup for pressure and net flow rate measurement of the microdiffuser. The fabricated microdiffusers are assembled with the piezoelectric actuator, thereby assembling the experimental apparatus of Fig.6(b) with the build-in pressure sensor arrays.

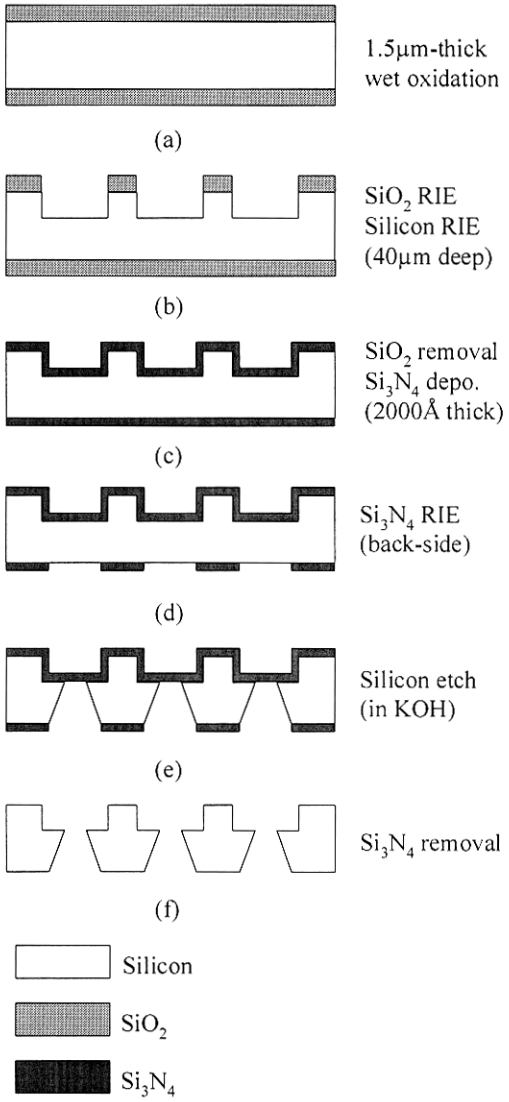

Figure 4. Fabrication process for the microdiffuser: (a) Growth of a 1.5μm-thick silicon dioxide layer on the 520μm-thick silicon wafer; (b) RIE of silicon dioxide layer, followed by RIE of 40μm-deep microdiffuser on the front-side of silicon wafer; (c) Removal of silicon dioxide layer, followed by LPCVD of a 2000Å-thick silicon nitride layer; (d) RIE of the backside silicon nitride layer; (e) KOH etching of the silicon substrate; (f) Wet etching of the silicon nitride layer.

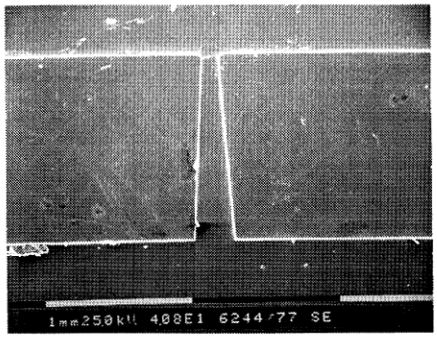

Figure 5. SEM of the fabricated microdiffuser.

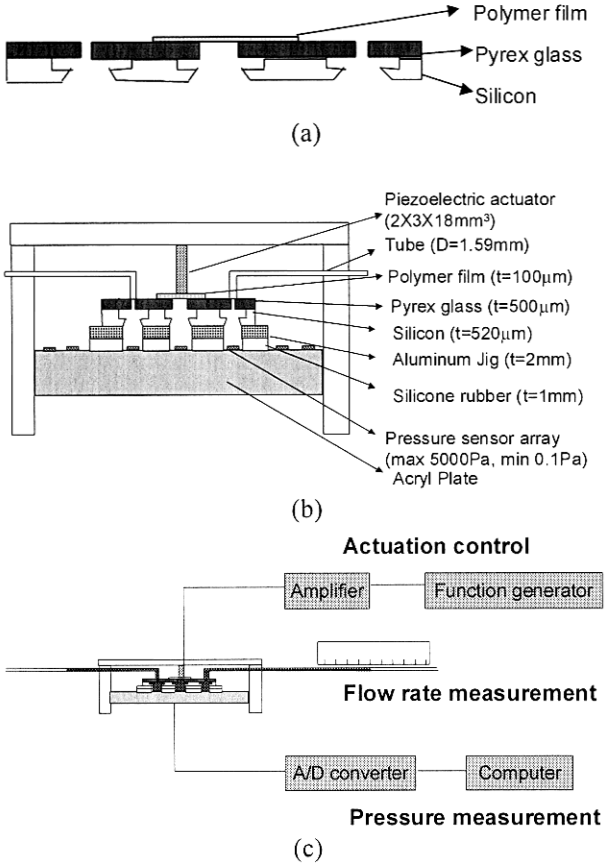

Figure 6. Experimental Apparatus: (a) Microdiffuser assembly; (b) Assembly of experimental apparatus; (c) Setup of test instruments.

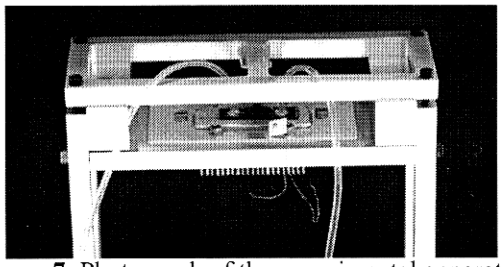

Figure 7. Photograph of the experimental apparatus.

Thus, when amplified AC signal is supplied to the piezoelectric actuator, the polymer film moves up- and downward. The supplied signals are 20, 40, 60, 100 Vp-p sinusoidal waves, respectively. We use water as a working fluid passing through the microdiffuser. In order to remove the air bubbles in the chamber and diffuser, we pass CO_2 gas through the chamber as well as the assembled microdiffusers for 20minutes before we fill the chamber and microdiffusers with water. Due to the high solubility of the CO_2 gas in the water, we complete the water charging process without residual bubbles.

We use a flexible Tygon® tube whose inner diameter is 1.59mm in order to estimate the net flow rate by measuring the distance the water moved through a tube (Fig. 6(c)) and we also use a pressure sensor array to measure the chamber pressure. Figure 7 shows the photograph of the assembled experimental apparatus.

EXPERIMENTAL RESULTS

We measure the net flow rate as well as the inlet, outlet and chamber pressures of the microdiffusers using the experimental apparatus of Figs.6 and 7. Figure 8 shows the net flow rate of D300. The prototypes, D100 and D300, show the maximum net flow rates of 116.6μl/min and 344.4μl/min, respectively, for an identical piezoelectric actuation using the sinusoidal drive voltage of 100Vp-p at 50Hz. The maximum net flow rate for D300 is 2.95 times larger than that for the D100, because the neck width of D300 is 3 times larger than that of D100.

The measured pressures of inlet chamber and outlet chamber is almost same as the atmospheric pressure, thus we can approximate the pressure difference between microdiffuser inlet and outlet as the pressure of pumping chamber. Figure 9 shows measured pressure difference of D300. The maximum pressure difference is about 1.6kPa for a piezoelectric actuation using the sinusoidal drive voltage of 100Vp-p at 50Hz. Unlike the net flow rate, the pressure difference of diffuser D300 is about the same as diffuser D100.

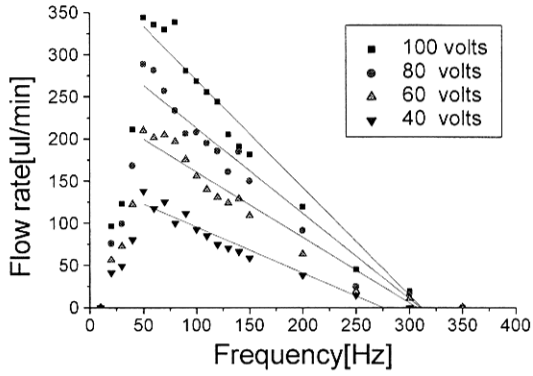

Figure 8. Measured net flow rate of D300.

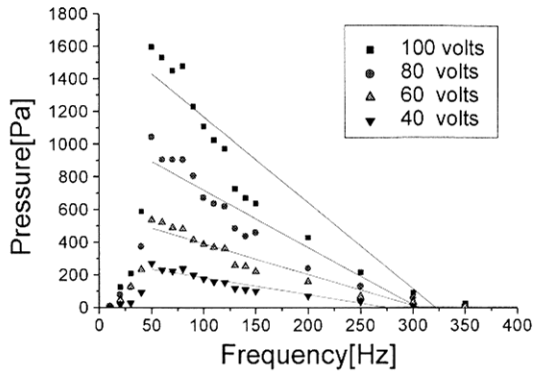

Figure 9. Measured pressure difference of D300.

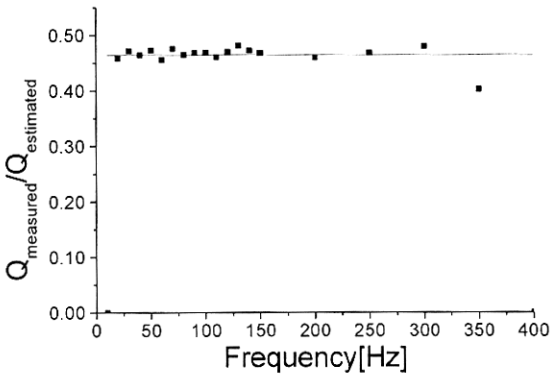

Figure 10. The measured net flow rate, normalized by the estimated values for D100.

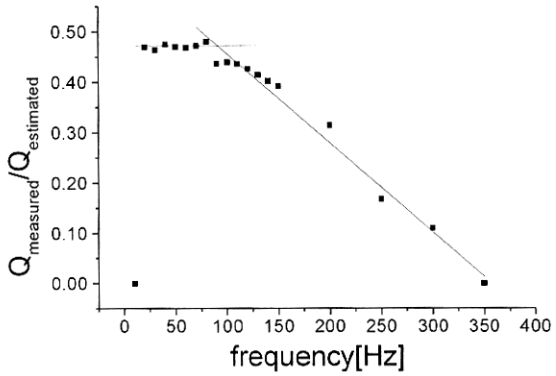

Figure 11. The measured net flow rate, normalized by the estimated values for D300.

Figure 10 illustrates that, for D100, the experimental flow rates are smaller than the theoretical values estimated from the static diffuser flow at a constant reduction ratio of 46.5±6.23% in the flow frequency range of 20~350Hz. The reason for the difference between the measured net flow rate and the estimated flow rate is that the estimated flow rate is based on uni-directional and turbulent flow. In our experiment, the flow in the microdiffuser is bi-directional and the maximum Reynolds number is estimated as 290, thus the flow is laminar.

Our dynamic flow model estimates that the net flow rates in the microdiffuser of D100 starts to decrease at the bi-directional flow frequencies greater than 500Hz, at which the total boundary layer thickness becomes the neck width of the microdiffusers. The constant ratio of the experimental flow rates to the theoretical values in Fig. 12 supports the validity of our dynamic flow model.

For the case of D300 (Fig.11), however, the experimental net flow rate starts to decrease over the bi-directional flow frequency of 90Hz, compared with the values estimated from the static flow model. The cut-off frequency of 90Hz in Fig. 11 supports our dynamic flow model where that the boundary layer thickness decreases to the microdiffuser neck width at the bi-directional flow frequency of 75Hz. The reason for the discrepancy between the measured 90Hz and the estimated 75Hz is that we assumed the boundary layer thickness of the microdiffuser is very close to that from the Stokes' second problem and neglected the variation of the boundary layer thickness due to the microdiffuser geometry.

Consequently, it is concluded that, as we expected in our dynamic flow model, the flow rectification performance and net flow capability of the microdiffuser valves tend to reduce when the total boundary layer thickness is smaller than the neck width of the microdiffuser.

CONCLUSIONS

We characterized the bi-directionally oscillating dynamic flow in the planar microdiffuser and evaluated the frequency-dependent flow rectification performance of the microdiffuser. In the theoretical study, we presented the theoretical model for the bi-directionally oscillating flow in the planar microdiffuser, where the neck width and boundary layer thickness governs the rectification performance of the microdiffuser. From the experimental study, we found that the net flow rates measured for the low-frequency bi-directional flow in the microdiffusers are approximately 47% of the values estimated from the uni-directional flow model. We also found that the net flow rates measured for the high-frequency bi-directional flow are rapidly decreased from those measured in low-frequency flow. It is concluded that, for high rectification performance of the microdiffuser that the neck width of the microdiffuser has to be lager than twice of the boundary layer thickness in the range of the operating frequency of the micropump.

REFERENCES

[1] M. A. Huff, M. S. Mettner, T. A. Lober and M. A. Schemidt, "A Pressure-Balanced Electrostatically-Activated Microvalves," *Proc. IEEE Solid-State Sensor and Actuator Workshop*, Hilton Head Island, South Carolina, 1990, pp.123-127.

[2] H. Jerman, "Electrically-Activated Micromachined Diaphragm Valves," *Proc. IEEE Solid-State Sensor and Actuator Workshop*, Hilton Head Island, South Carolina, 1990, pp.65-69.

[3] K. Yanagisawa, H. Kuwano and A. Tago, "An Electromagnetically Driven Microvalve," *Proc. 1993 Int. Conf. on Solid-State Sensors and Actuators (Transducers '93)*, Yokohama, Japan, 1993, pp.102-105.

[4] J. Behrens, A. Meckes and W. Benecke, "Micropump and -Valves with Electromagnetic Actuation," *Micro System Technologies 96*, Potsdam, Germany, 1996, pp.820-822.

[5] Meckes, J. Behrens and W. Benecke, "A Microvalve with Electromagnetic Actuator," *Actuators 98*, Bremen, Germany, 1998, pp.152-155.

[6] E. Stemme, G. Stemme, " A Valveless Diffuser/Nozzle–based Fluid Pump," *Sensors and Actuator*, A39(1993) 159-167.

[7] T. Gerlach, "Microdiffuser as Dynamic Passive Valves for Micropump Applications," *Sensors and Actuators*, A69(1998) 181-191.

[8] Olsson, G. Stemme, E. Stemme, " Micromachined Diffuser/Nozzle Elements for Valveless Pumps," *Proc. Micro Elctro Mechanical Systems Workshop*, San Diego, California, 1996, pp. 378-383.

[9] Olsson, G. Stemme, E. Stemme, "An Improved Valveless Pump Fabricated using Deep Reactive Ion Etching," *Proc. Micro Elctro Mechanical Systems Workshop*, San Diego, California, 1996, pp. 479-484.

[10] S. Shoji, "Fluids for Sensor Systems," *Topics in Current Chemistry*, Vol.194 (1998) 163-188.

[11] T. S. J. Lammerink, M. Elwenspoek and J. H. J. Fluitman, "Integrated Micro-Liquid Dosing System," *Proc. Micro Electro Mechanical Systems Workshop*, Fort Lauderdale, Florida, 1993, pp.245-59.

[12] J. A. Schetz, A. E. Fuhs, *Handbook of fluid dynamics and fluid machinery*, John Willy & Sons, 1996, pp. 2024-2027.

[13] G. Currie, *Fundamental Mechanics of Fluids*, McGraw-Hill, 1993, pp. 228-230.

[14] H. Schlichting, *Boundary Layer Theory*, McGraw-Hill, 1979, pp. 436-438.